

# Simple analytical approximations for treatment of inverse Compton scattering of relativistic electrons in the black-body radiation field

D. Khangulyan

*Institute of Space and Astronautical Science/JAXA,  
3-1-1 Yoshinodai, Chuo-ku, Sagami-hara, Kanagawa 252-5210, Japan*  
khangul@astro.isas.jaxa.jp

F.A. Aharonian

*Dublin Institute for Advanced Studies, 31 Fitzwilliam Place, Dublin 2, Ireland; Max-Planck-Institut für Kernphysik, Saupfercheckweg 1, D-69117 Heidelberg, Germany*  
Felix.Aharonian@mpi-hd.mpg.de

S.R. Kelner

*Max-Planck-Institut für Kernphysik, Saupfercheckweg 1, D-69117 Heidelberg, Germany; National Research Nuclear University, Kashira Hwy 31, 115409 Moscow, Russia*  
Stanislav.Kelner@mpi-hd.mpg.de

## ABSTRACT

The inverse Compton (IC) scattering of relativistic electrons is one of the major gamma-ray production mechanisms in different environments. Often the target photons for the IC scattering are dominated by black (or grey) body radiation. In this case, the precise treatment of the characteristics of IC radiation requires numerical integrations over the Planckian distribution. Formally, analytical integrations are also possible but they result in series of several special functions; this limits the efficiency of usage of these expressions. The aim of this work is the derivation of approximate analytical presentations which would provide adequate accuracy for the calculations of the energy spectra of up-scattered radiation, the rate of electron energy losses, and the mean energy of emitted photons. Such formulae have been obtained by merging the analytical asymptotic limits. The coefficients in these expressions are calculated via the least square fitting of the results of numerical integrations. The simple analytical presentations, obtained for both the isotropic and anisotropic target radiation fields, provide adequate (as good as 1%) accuracy for broad astrophysical applications.

*Subject headings:* radiation mechanisms: non-thermal – methods: analytical – gamma rays: general – gamma rays: stars

## 1. Introduction

Relativistic electrons can transfer their energy to gamma rays through the process of inverse Compton (IC) scattering of the ambient low energy photons. Together with bremsstrahlung, this

process represents a major channel of gamma-ray production by relativistic electrons (and positrons). At energies below 100 MeV, a non-negligible contribution to the gamma-ray continuum can be supplied by annihilation of positrons on flight. In the same energy band, one may ex-

pect a contribution from the synchrotron radiation of electrons. However, the latter scenario can be effectively realized only in quite unique objects called extreme accelerators, when the particle acceleration proceeds at the maximum (theoretically possible) rate. In general, the synchrotron radiation is released well below the gamma-ray band, and, in fact, is considered as a dissipative process as long as it concerns the efficiency of gamma-ray production. Indeed, in environments with the energy density of the magnetic field significantly exceeding the energy density of the radiation field,  $f = B^2/(8\pi w_{\text{rad}}) \gg 1$ , only a small fraction ( $f^{-1}$ ) of the kinetic energy of electrons is released in high energy gamma rays. Otherwise, the radiative cooling of electrons is dominated by the IC scattering, making the latter an extremely effective gamma-ray production mechanism, especially at very high energies, when the radiative cooling due to bremsstrahlung is suppressed compared to the IC scattering<sup>1</sup>. Because of the large cross-section of the process and the presence of high density radiation fields, the IC scattering undoubtedly is the most prolific and universal gamma-radiation mechanism which contributes from low (MeV) to ultrahigh (tens of TeV) energies of emission of almost all nonthermal source populations - supernova remnants (SNR), pulsar wind nebulae (PWNe), compact binary systems, active galactic nuclei, *etc.*

The energy spectrum of the up-scattered photons depends strongly on the energy of target photon, especially in the Thomson regime, when the average energy of the up-scattered photon is proportional to the energy of the target photon. In the Klein-Nishina regime, the most fraction of the electron energy is transferred to the up-scattered photon, thus the dependence on the target photon energy gradually disappears. Given this nontrivial dependence on the target photon energy, the accurate calculations of the IC spectrum require good knowledge of the energy distribution of target photons. Fortunately, in many cases the dominant contribution to the IC scattering comes from photons belonging to black-body (or grey-body) radiation, i.e. they are described by the standard

<sup>1</sup>This follows from the ratio of the cooling times due to the bremsstrahlung and IC scattering (in the Thomson regime):  $t_{\text{br}}/t_{\text{IC}} \propto E \times (N_{\text{gas}}/w_{\text{rad}})$ , where  $E$  is the electron's energy, and  $N_{\text{gas}}$  is the gas density.

Planckian distribution:

$$dN_{\text{ph}} \propto \frac{\omega_0^2 d\omega_0}{e^{\omega_0/T} - 1}, \quad (1)$$

where  $T$  and  $\omega_0$  are the photon gas temperature and the photon energy, respectively (hereafter the energies of both photons and electrons, as well as the photon gas temperature, are expressed in units of  $m_e c^2$ ).

Planckian distribution is realized in the case of IC scattering on the 2.7 K cosmic microwave background radiation (CMBR). Remarkably, in SNRs and PWNe in our Galaxy, as well as in extragalactic objects like large scale AGN jets and Clusters of galaxies, the IC scattering in the VHE band is strongly dominated by CMBR. The target photons for the IC scattering can be well described by the Planckian distribution also in compact systems like gamma-ray emitting binaries containing either a pulsar (binary pulsars) or a black hole (microquasars). Despite the different origins of the nonthermal energy, supported in the first case by a rotation-powered pulsar wind, and in the second case by an accretion-powered jet, the most likely mechanism of gamma-radiation is the IC scattering. In both type of objects the target photons are supplied by the thermal radiation of the bright optical star. Finally, in some cases quite complex photon distributions can be represented as a superposition of several grey-body components.

Since the Planckian distribution of photons is characterized by a rapid decrease of the density both at low and at high energies, numerical integrations of the Compton cross section over the Planckian photon field generally do not impose computational difficulties, but simply require additional computational time. Often, to shorten the calculations, different approximations are used. The most common approach is the  $\delta$ -functional approximation for the narrow Planckian spectrum. This approximation can correctly describe the lower energy part of the spectrum, but is not applicable for the precise computations of the entire gamma-ray spectra (see Section 6). Therefore, some other approximations for calculations of IC spectra have been recently suggested in the literature (see Petruk 2009; Zdziarski & Pjanka 2013). These approaches provide a better description for the IC spectra and are characterized by a higher precision than the  $\delta$ -functional approxi-

mation does, although they are not free of certain limitations (see discussion in Section 6).

In this paper we propose new, very simple analytical presentations obtained for both isotropic and mono-directional angular distributions of target radiation field assuming that its energy spectrum is precisely described by the Planckian distribution. We provide analytical formulae for the energy spectra of upscattered radiation, as well as for the interaction and the energy-loss rates of electrons. The “threshold” for the accuracy of these formulae in all cases has been set at the level of 1%.

## 2. Approximate description of the IC process

The interaction of electrons with photons is described with the standard means of quantum electrodynamics. In the astrophysical context, the general expressions for the Compton cross-section can be significantly simplified using the fact that the energy of the target photons is typically small,  $\omega_0 \ll 1$ , and the electrons are relativistic,  $E \gg 1$  (this condition, in particular, implies that the upscattered photon moves in the direction of the initial velocity of the electron). Under these circumstances, for the target photons with a fixed direction, the scattering rate by an electron moving with a velocity which makes an angle  $\theta$  with the photon’s direction has the following simple form (Aharonian & Atoyan 1981):

$$\begin{aligned} \frac{d\nu_{\text{ani}}}{d\omega dN_{\text{ph}} dt} &= c(1 - \cos\theta) \frac{d\sigma}{d\omega} \\ &= \frac{4\pi cr_0^2(1 - \cos\theta)}{b_\theta E} \times \\ &\left[ 1 + \frac{z^2}{2(1-z)} - \frac{2z}{b_\theta(1-z)} + \frac{2z^2}{b_\theta^2(1-z)^2} \right], \end{aligned} \quad (2)$$

where  $E$ ,  $\omega_0 = b_\theta/[2E(1 - \cos\theta)]$  and  $\omega = zE$  are energies of electron, soft photon, and upscattered photon, respectively;  $r_0 = e^2/(m_e c^2)$  is the electron classical radius; and  $N_{\text{ph}}$  is number of target photons per unit of volume. If the target photon field is isotropic, the above expression should be averaged over the interaction angle (Aharonian & Atoyan 1981):

$$\begin{aligned} \frac{d\nu_{\text{iso}}}{d\omega dN_{\text{ph}} dt} &= c \int (1 - \cos\theta) \frac{d\sigma}{d\omega} \frac{d\Omega}{4\pi} \\ &= \frac{8\pi cr_0^2}{bE} \times \\ &\left[ 1 + \frac{z^2}{2(1-z)} + \frac{z}{b(1-z)} - \frac{2z^2}{b^2(1-z)^2} - \right. \\ &\left. \frac{z^3}{2b(1-z)^2} - \frac{2z}{b(1-z)} \log \frac{b(1-z)}{z} \right], \end{aligned} \quad (3)$$

where  $b = 4\omega_0 E$  is the Klein-Nishina parameter and the notation  $\log$  is used for logarithm to the base  $e$ , i.e. “natural logarithm”. Note that Equation (3) has been originally derived by Jones (1968) in a straight way, without using the intermediate angle-dependent rate given by Equation (2) (for a review see Blumenthal & Gould 1970).

In the case of black-body target photons, the scattering rates given by Equations (2) and (3) should be integrated over the Planckian distribution of target photons:

$$dN_{\text{ph}} = \frac{m_e^3 c^3 \kappa}{\pi^2 \hbar^3} \frac{\omega_0^2 d\omega_0}{e^{\omega_0/T} - 1}, \quad (4)$$

where  $\kappa$  is the dilution factor in the case of grey-body radiation. The lower integration limit,  $\omega_0 \geq \epsilon_{\text{ani/iso}}$ , is determined by the kinematic conditions (i.e., conditions imposed by the conservation of 4-momentum) as

$$\epsilon_{\text{ani}} = \frac{\omega}{2E} \frac{1}{(E - \omega)} \frac{1}{(1 - \cos\theta)} = \frac{z}{1 - z} \frac{T}{t_\theta} \quad (5)$$

and

$$\epsilon_{\text{iso}} = \frac{\omega}{4E} \frac{1}{(E - \omega)} = \frac{z}{1 - z} \frac{T}{t} \quad (6)$$

for the cases of mono-directional and isotropic photon distributions, respectively. Here, the following notations are used:  $t_\theta = 2ET(1 - \cos\theta)$  and  $t = 4ET$ .

Formally, for large values of  $\omega_0 \rightarrow +\infty$ , Equations (2) and (3) are not applicable, since the basic assumption,  $\omega_0 \ll \omega$ , used for the derivation of these expressions fails. However, assuming a non-relativistic photon temperature  $T \ll 1$ , one can safely extend the integration upper limit to  $+\infty$ . Therefore, the interaction rate with black-body distribution of target photons is

$$\frac{dN_{\text{ani/iso}}}{d\omega dt} = \frac{T^3 m_e^3 c^3 \kappa}{\pi^2 \hbar^3} \int_{\epsilon_{\text{ani/iso}}/T}^{\infty} \frac{d\nu_{\text{ani/iso}}}{d\omega dN_{\text{ph}} dt} \frac{x^2 dx}{e^x - 1}. \quad (7)$$

The substitution of Equations (2) and (3) into Equation (7) leads to an expression that can be presented in the form which contains the following functions introduced by Zdziarski & Pjanka (2013) (Equations (15) and (29) in their paper):

$$f_i = \int_{x_0}^{\infty} \frac{x^i dx}{e^x - 1}, \quad (8)$$

for  $i = -1, 0$  and  $+1$ ; and

$$f_{\text{ln}} = \int_{x_0}^{\infty} \frac{\log(x) dx}{e^x - 1}. \quad (9)$$

While the integral  $f_0$  is expressed through elementary functions:

$$f_0 = -\log(1 - e^{-x_0}), \quad (10)$$

and  $f_{+1}$  allows a representation with the dilogarithm function (see Equation(7) of Zdziarski & Pjanka 2013), the two other functions ( $f_{-1}$  and  $f_{\text{ln}}$ ), as shown by Zdziarski & Pjanka (2013), can be expressed through series (Equation (14, 28) of Zdziarski & Pjanka 2013). However, each of these terms contains special functions, which makes the usage of these expressions rather inconvenient.

We use a different approach to obtain approximate formulae for the IC cross-section. First, we present the cross-section in a form containing strictly positive terms. This dramatically reduces the risk of large mistakes because of the summation of rounding errors. Furthermore, we approximate these terms by simple analytical expressions. The derivations of these expressions are based on analytical computations of the asymptotic limits and the introduction of correction functions for the intermediate range of energies by invoking a least square fit. This allows us to present Equation (7) in a form that contains only elementary functions.

For the case of a mono-directional photon field, Equation (7) can be expressed as:

$$\frac{dN_{\text{ani}}}{d\omega dt} = \frac{2r_o^2 m_e^3 c^4 \kappa T^2}{\pi \hbar^3 E^2} \times \left[ \frac{z^2}{2(1-z)} F_1(x_0) + F_2(x_0) \right], \quad (11)$$

where  $x_0 = \frac{z}{(1-z)t\theta}$ , and the positive functions  $F_1$  and  $F_2$  are determined as:

$$F_1(x_0) = f_{+1}(x_0), \quad (12)$$

$$F_2(x_0) = f_{+1}(x_0) + 2x_0^2 f_{-1}(x_0) - 2x_0 f_0(x_0). \quad (13)$$

For the case of an isotropic photon field, Equa-

tion (7) obtains the following form:

$$\frac{dN_{\text{iso}}}{d\omega dt} = \frac{2r_o^2 m_e^3 c^4 \kappa T^2}{\pi \hbar^3 E^2} \times \left[ \frac{z^2}{2(1-z)} F_3(x_0) + F_4(x_0) \right], \quad (14)$$

where  $x_0 = \frac{z}{(1-z)t}$ . The positive functions  $F_3$  and  $F_4$  are expressed via  $f_{-1}$ ,  $f_0$ ,  $f_{+1}$  and  $f_{\text{ln}}$ :

$$F_3(x_0) = f_{+1}(x_0) - x_0 f_0(x_0); \quad (15)$$

and

$$F_4(x_0) = \left( f_{+1}(x_0) - x_0 f_0(x_0) \right) + 2x_0 \left( \log(x_0) f_0(x_0) - f_{\text{ln}}(x_0) \right) + 2x_0 \left( f_0(x_0) - x_0 f_{-1}(x_0) \right). \quad (16)$$

Thus, the IC radiation spectra can be presented in simple analytical forms of Equations (11) and (14) as functions of the variable  $z$  through the term  $z^2/(2(1-z))$  and four functions  $F_1$ ,  $F_2$ ,  $F_3$  and  $F_4$ . All these functions depend only on the parameter  $x_0$ , which is equal to  $z/((1-z)t\theta)$  and  $z/((1-z)t)$  in the case of mono-directional and isotropic photon fields, respectively.

The functions  $F_1$  and  $F_2$  have the same asymptotic limits:

$$F_{1,2} = \begin{cases} \frac{\pi^2}{6}, & x_0 \ll 1 \\ x_0 e^{-x_0}, & x_0 \gg 1 \end{cases}. \quad (17)$$

A simple function with the similar asymptotic behavior can be used as a zeroth-order approximation for the functions  $F_1$  and  $F_2$  (see Figure 1):

$$G_{1,2}^{(0)} = \left( \frac{\pi^2}{6} + x_0 \right) e^{-x_0}. \quad (18)$$

A numerical comparison of these functions shows that  $G_1^{(0)}$  provides<sup>2</sup> accuracy of 10% and 50% for  $F_1$  and  $F_2$ , respectively. To improve the accuracy, we introduce correction functions:

$$G_{1,2} = G_{1,2}^{(0)}(x_0) \times g_{1,2}(x_0), \quad (19)$$

<sup>2</sup>The functions  $G_1^{(0)}$  and  $G_2^{(0)}$  are identical.

We present the correction factors  $g_1$  and  $g_2$  as functions of the variable  $x_0$  with four free parameters:

$$g_i(x_0) = \left[ 1 + \frac{a_i x_0^{\alpha_i}}{1 + b_i x_0^{\beta_i}} \right]^{-1}. \quad (20)$$

The parameters  $\alpha_i > 0, a_i, \beta_i > \alpha_i, b_i > 0$  were used for the least-square fitting of functions  $F_{1,2}$ . Obviously, this is not a unique representation for the approximation function, but since  $g \rightarrow 1$  for  $x \ll 1$  and  $x \gg 1$ , the considered function family should preserve the asymptotic behavior of the zeroth-order fit  $G_{1,2}^{(0)}$  and provide enough freedom for fitting. We therefore use Equation (20) as the correction function for fitting procedures used in this paper.

The numerical least square fitting gives the following sets of parameters

$$\begin{aligned} \alpha_1 &= 0.857, & a_1 &= 0.153, \\ \beta_1 &= 1.84, & b_1 &= 0.254; \end{aligned} \quad (21)$$

and

$$\begin{aligned} \alpha_2 &= 0.691, & a_2 &= 1.33, \\ \beta_2 &= 1.668, & b_2 &= 0.534, \end{aligned} \quad (22)$$

which provide a precision of better than 1% for the entire range of  $x_0$ , as shown in Figures 2 and 3.

A similar approach can be used for the approximation of the angle averaged IC spectra determined by Equation (14). The functions  $F_3$  and  $F_4$  have the same asymptotic:

$$F_{3,4} = \begin{cases} \frac{\pi^2}{6}, & x_0 \ll 1 \\ e^{-x_0}, & x_0 \gg 1 \end{cases}, \quad (23)$$

which suggests the following family of approximation functions:

$$G_{3,4} = G_{3,4}^{(0)}(x_0) \times g_{3,4}(x_0), \quad (24)$$

where

$$G_{3,4}^{(0)}(x_0) = \frac{\pi^2}{6} \frac{1 + c_{3,4} x_0}{1 + \frac{\pi^2 c_{3,4}}{6} x_0} e^{-x_0}. \quad (25)$$

The functions  $G_{3,4}^{(0)}$  have a similar asymptotic behavior as the functions  $F_{3,4}$ ; it is demonstrated in Figure 4. Here  $c_{3,4} > 0$  are parameters which do not change the asymptotic behavior of  $G_{3,4}^{(0)}$ .

Therefore, they can be optimized for a better description of functions  $F_{3,4}$ . In particular, for the value of  $c_3 = 2.73$  the function  $G_3^{(0)}$  provides a 3% accuracy for the function  $F_3$ , as shown in Figure 4.

As can be seen in Figure 4, the function  $F_4 \times e^{x_0}$  features a  $\sim 30\%$  dip at  $x_0 \sim 1$ , which cannot be reproduced by the function  $G_4^{(0)}$ . Therefore the parameter  $c_4$  alone cannot provide an approximation with precision better than a 30% for the function  $F_4$  (such accuracy can be achieved for  $c_4 \simeq 50$ ). However, Equation (24) provides a five-parameter ( $a_{3,4}, \alpha_{3,4}, b_{3,4}, \beta_{3,4}$  and  $c_{3,4}$ ) function family that can be used for fitting functions  $F_{3,4}$ . The numerical least-square fits resulted in the following sets of parameters

$$\begin{aligned} \alpha_3 &= 0.606, & a_3 &= 0.443, \\ \beta_3 &= 1.481, & b_3 &= 0.54, \\ & & c_3 &= 0.319; \end{aligned} \quad (26)$$

and

$$\begin{aligned} \alpha_4 &= 0.461, & a_4 &= 0.726, \\ \beta_4 &= 1.457, & b_4 &= 0.382, \\ & & c_4 &= 6.62, \end{aligned} \quad (27)$$

which gave a  $< 1\%$  precision for the entire range of  $x_0$ , as shown in Figures 5 and 6.

The parameterizations for the functions  $F_1, F_2, F_3, F_4$  given by Equations (19) and (24), with corresponding parameters from Equations (21–22) and (26–27), allow us to describe the IC spectra, Equations (11) and (14), with a precision better than 1%. Note that this value corresponds to the maximum deviation of the approximate formulae from the precise value; in the case of a broad distribution of electrons, the accuracies obviously will be significantly better.

The obtained above approximations describe the IC spectra for two different, isotropic and mono-directional angular distributions of target photons. The former scenario with an involvement of CMBR is often realized in different objects like SNRs, PWNe, and Clusters of Galaxies. However, in many other cases the background photon field can be approximated as a grey-body (or a superposition of a several grey-body components) emission. In this case the energy,  $\omega_*$ , at which the spectral energy distribution (i.e.,  $\nu F_\nu$ ) of target photons achieves the maximum, allows to define the temperature of the grey-body emission:

$$T = 0.255 \omega_*. \quad (28)$$

The energy density of the target photon field,  $w_*$ , allows then to obtain the corresponding dilution coefficient:

$$\kappa = 360 \frac{\hbar^3 w_*}{m_e^3 c^5} \left( \frac{\omega_*}{m_e c^2} \right)^{-4}. \quad (29)$$

The approximation of a mono-directional photon field is applicable when the source of the target photons is compact, namely in the IC production region the value of  $(1 - \cos \theta)$  should not vary significantly for the photons coming from different regions of the source. Then in the IC production site, the target photon field is typically diluted by a factor

$$\kappa = \frac{\Delta\Omega}{4\pi}, \quad (30)$$

where  $\Delta\Omega \ll 1$  is the solid angle of the target photons' source, as seen from the IC production region. In case the source of target photons is a star, Equation (30) can be expressed through the radius,  $R_*$ , of the star and distance,  $R$ , between the IC emitter and the star (the condition  $\Delta\Omega \ll 1$  is realized if  $R \gg R_*$ ):

$$\kappa = \left( \frac{R_*}{2R} \right)^2. \quad (31)$$

### 3. The rate of IC losses

IC energy losses of a particle in a Planckian photon field can be expressed as

$$\dot{E}_{\text{ani/iso}} = \frac{m_e^3 c^3 \kappa E^2}{\pi^2 \hbar^3} \times \int_0^\infty d\omega_0 \frac{\omega_0^2}{e^{\omega_0/T} - 1} \int_0^{z_{\text{max}}} dz z \frac{d\nu_{\text{ani/iso}}}{d\nu dN_{\text{ph}} dt}, \quad (32)$$

where  $z_{\text{max}}$  is  $\frac{b}{1+b}$  or  $\frac{b_\theta}{1+b_\theta}$  for isotropic and mono-directional photon fields, respectively. Formally, the integration lower limit is not equal to 0, however the contribution to the integral from the region of small  $z$  is negligible. Therefore we formally set the lower limit to 0.

The structure of Equation (32) allows us to determine the dependence of the energy-loss rate on the electron energy and photon field temperature. Namely, if the IC scattering proceeds with a fixed

interaction angle, one obtains

$$\begin{aligned} \dot{E}_{\text{ani}} &= \frac{r_0^2 m_e^3 c^4 \kappa}{2\pi \hbar^3 (E(1-\cos\theta))^2} \int_0^\infty db_\theta \frac{b_\theta}{e^{b_\theta/T_\theta} - 1} \times \\ &\int_0^{\frac{b_\theta}{(1+b_\theta)}} dz z \left[ 1 + \frac{z^2}{2(1-z)} - \frac{2z}{b_\theta(1-z)} + \frac{2z^2}{b_\theta^2(1-z)^2} \right] \\ &= \frac{2r_0^2 m_e^3 c^4 \kappa T^2}{\pi \hbar^3} F_{\text{ani}}(t_\theta). \end{aligned} \quad (33)$$

Based on the asymptotic behavior of the function  $F_{\text{ani}}$

$$F_{\text{ani}}(u) = \begin{cases} \frac{\pi^4}{45} u^2 = 2.16u^2, & u \ll 1 \\ \frac{\pi^2}{12} \log(u) = 0.822 \log(u), & u \gg 1 \end{cases}, \quad (34)$$

we suggest the following approximate presentation for the function  $F_{\text{ani}}$

$$G_{\text{ani}}^{(0)}(u) = \frac{c_{\text{ani}} u \log(1 + 2.16u/c_{\text{ani}})}{1 + c_{\text{ani}} u/0.822}. \quad (35)$$

Least square fitting for the parameter  $c_{\text{ani}}$  results in  $c_{\text{ani}} = 6.13$ , for which Equation (35) provides accuracy of an order of 1% (see Figure 7).

Similarly, if IC cooling proceeds with isotropized scattering angles, the energy loss rate is

$$\begin{aligned} \dot{E}_{\text{iso}} &= \frac{r_0^2 m_e^3 c^4 \kappa}{8\pi \hbar^3 E^2} \int_0^\infty db \frac{b}{e^{b/T} - 1} \times \\ &\int_0^{\frac{b}{(1+b)}} dz z \left[ 1 + \frac{z^2}{2(1-z)} + \frac{z}{b(1-z)} - \right. \\ &\left. \frac{2z^2}{b^2(1-z)^2} - \frac{z^3}{2b(1-z)^2} - \frac{2z}{b(1-z)} \log \frac{b(1-z)}{z} \right] \\ &= \frac{2r_0^2 m_e^3 c^4 \kappa T^2}{\pi \hbar^3} F_{\text{iso}}(t). \end{aligned} \quad (36)$$

The asymptotic behavior of function  $F_{\text{iso}}$  is similar to Equation (34):

$$F_{\text{iso}}(u) = \begin{cases} \frac{\pi^4}{135} u^2 = 0.722u^2, & u \ll 1 \\ \frac{\pi^2}{12} \log(u) = 0.822 \log(u), & u \gg 1 \end{cases}, \quad (37)$$

Therefore, we can use a function similar to Equation (35):

$$G_{\text{iso}}^{(0)}(u) = \frac{c_{\text{iso}} u \log(1 + 0.722u/c_{\text{iso}})}{1 + c_{\text{iso}} u/0.822}. \quad (38)$$

Least square fitting for this function renders a value of  $c_{\text{iso}} = 4.62$ , for which Equation (38) pro-

vides a  $\sim 5\%$  precision (see Figure 7). This approximation can be improved by using the correction function defined by Equation (20). In particular, a set of the parameters

$$\begin{aligned}\alpha_{\text{iso}} &= 0.682, & a_{\text{iso}} &= -0.362, \\ \beta_{\text{iso}} &= 1.281, & b_{\text{iso}} &= 0.826, \\ & & c_{\text{iso}} &= 5.68\end{aligned}\quad (39)$$

provide a  $\sim 1\%$  precision (see Figure 7). A similar expression (although less optimized, with an accuracy of 3%) was originally presented in Bosch-Ramon & Khangulyan (2009).

The obtained Equation (35) for  $F_{\text{ani}}$  and Equations (38 – 39) for  $F_{\text{iso}}$  allow a precise description of the energy losses with formulae Equations (33) and (36), which correspond to the case of electron-photon interactions at a specific angle and angle averaged, respectively. It is important to note that the latter can be realized also in the cases when the target photons are mono-directional in the source frame. For example, if particles are isotropized by the source magnetic field, the production of the IC emission towards the observer proceeds at a specific interaction angle, since relativistic particles emit within a narrow cone towards the direction of their motion. However, if IC cooling time exceeds particle isotropization timescale, each particle can interact with photons at an arbitrary angle, therefore particle losses are effectively determined by the interaction with an isotropic photon field, i.e., by Equation (36).

The particle cooling described by Equation (33) can be realized, for example, in the so-called Compton-drag scenarios, i.e. when the temperature of the emitting particles is very small and the bulk motion component is dominant. In particular, this may be relevant to the pulsar-wind zone for pulsars located in systems with bright stars (see, e.g., Khangulyan et al. 2007, 2011). Also a similar situation can arise if IC cooling time is shorter than isotropization time-scale.

Often it is convenient to characterize the energy losses through the cooling-time:

$$t_{\text{ic}} = \frac{E}{\dot{E}} = \frac{\pi \hbar^3}{2r_0^2 m_e^3 c^4 \kappa T^2} \frac{E}{F_{\text{ani/iso}}(t_{\theta/})}. \quad (40)$$

In the Thomson limit, for the case of an isotropic

photon field, this expression gives:

$$t_{\text{ic}} = \left( \frac{4cE}{3} \frac{\pi^2 \kappa T^4 m_e^3 c^3}{15 \hbar^3} \frac{8\pi r_0^2}{3} \right)^{-1}, \quad (41)$$

where the middle term corresponds to the ratio of energy density of the black-body photon distribution to  $m_e c^2$ .

It was suggested in Aharonian et al. (2006) and further generalized by Bosch-Ramon & Khangulyan (2009) that, in the case of an isotropic photon field, IC cooling time in the Klein-Nishina limit can be described by a simple function:

$$t_{\text{ic}} \approx 5 \times 10^{-17} T^{-2.3} E^{0.7} \text{s}, \quad (42)$$

where we transformed the numerical coefficient from Equation (13) in Bosch-Ramon & Khangulyan (2009) to the units used in this paper, and adopted a dilution coefficient to be 1. The comparison of Equations (40) and (42) shows that the latter implies that function  $F_{\text{iso}}$  has been approximated as  $F_{\text{iso}} \simeq 0.4t^{0.3}$ , which provides an accuracy of  $< 30\%$  for  $5 < t < 10^3$ .

#### 4. Interaction rate

Another important characteristic of Compton scattering are the interaction rates:

$$\dot{N}_{\text{ani}} = \frac{m_e^3 c^4 \kappa}{\pi^2 \hbar^3} \int_0^\infty d\omega_0 \frac{\omega_0^2}{e^{\omega_0/T} - 1} (1 - \cos \theta) \sigma(b_\theta), \quad (43)$$

and

$$\dot{N}_{\text{iso}} = \frac{m_e^3 c^4 \kappa}{\pi^2 \hbar^3} \int_0^\infty d\omega_0 \frac{\omega_0^2}{e^{\omega_0/T} - 1} \int_{-1}^1 \frac{d \cos \theta}{2} (1 - \cos \theta) \sigma(b_\theta), \quad (44)$$

for the scattering at a fixed interaction angle, and for the angle averaged interactions, respectively. Here  $\sigma$  is the Lorentz-invariant cross section for Compton scattering (see e.g. Berestetskii et al. 1971):

$$\sigma(x) = \frac{2\pi r_0^2}{x} \times \left[ \left(1 - \frac{4}{x} - \frac{8}{x^2}\right) \log(1+x) + \frac{1}{2} + \frac{8}{x} - \frac{1}{2(1+x)^2} \right]. \quad (45)$$

For the case of fixed scattering angle, the interaction rate can be expanded as

$$\begin{aligned}\dot{N}_{\text{ani}} &= \frac{r_0^2 m_e^3 c^4 \kappa}{4\pi \hbar^3 E^3 (1 - \cos\theta)^2} \times \\ &\int_0^\infty db \theta \frac{b_\theta}{e^{b_\theta/t_\theta} - 1} \left[ \left(1 - \frac{4}{b_\theta} - \frac{8}{b_\theta^2}\right) \log(1 + b_\theta) + \right. \\ &\quad \left. \frac{1}{2} + \frac{8}{b_\theta} - \frac{1}{2(1+b_\theta)^2} \right] \\ &= \frac{2r_0^2 m_e^3 c^4 \kappa T^2}{\pi \hbar^3 E} F_{\text{n,ani}}(t_\theta) .\end{aligned}\quad (46)$$

The integral term in Equation (46) has the following asymptotic behavior<sup>3</sup>:

$$F_{\text{n,ani}}(u) = \begin{cases} \frac{4}{3}\zeta(3)u = 1.6u, & u \ll 1 \\ \frac{\pi^2}{12} \log(u) = 0.822 \log(u), & u \gg 1 \end{cases}, \quad (47)$$

therefore in the zeroth-order approximations this function can be presented in the form:

$$G_{\text{n,ani}}^{(0)}(u) = 0.822 \log(1 + 1.95u) . \quad (48)$$

Like in the previous cases, one can improve this approximate formula by the correction function given in Equation (20). In Figure 8, we show  $G_{\text{n,ani}}^{(0)}(u) \times g(u)$  for the following parameter values:

$$\begin{aligned}\alpha_{\text{n,ani}} &= 0.885, & a_{\text{n,ani}} &= 1.05, \\ \beta_{\text{n,ani}} &= 1.213, & b_{\text{n,ani}} &= 2.46\end{aligned}\quad (49)$$

It can be seen that this approximation provides a precision at the level of 1%.

If the photon field is isotropic, the interaction rate can be expressed as

$$\begin{aligned}\dot{N}_{\text{iso}} &= \frac{r_0^2 m_e^3 c^4 \kappa}{16\pi \hbar^3 E^3} \int_0^\infty \frac{db}{e^{b/t} - 1} \times \\ &\int_0^b dx \left[ \left(1 - \frac{4}{x} - \frac{8}{x^2}\right) \log(1 + x) + \frac{1}{2} + \frac{8}{x} - \frac{1}{2(1+x)^2} \right] \\ &= \frac{2r_0^2 m_e^3 c^4 \kappa T^2}{\pi \hbar^3 E} F_{\text{n,iso}}(t) .\end{aligned}\quad (50)$$

Here the integral term has properties similar to Equation (47):

$$F_{\text{n,iso}}(u) = \begin{cases} \frac{2}{3}\zeta(3)u = 0.801u, & u \ll 1 \\ \frac{\pi^2}{12} \log(u) = 0.822u, & u \gg 1 \end{cases}, \quad (51)$$

Thus, in the zeroth-order approximation this function can be presented as

$$G_{\text{n,iso}}^{(0)}(u) = 0.822 \log(1 + 0.97u) . \quad (52)$$

This approximation provides relatively poor precision (at the level of < 30%). However, adopting the correction function given in Equation (20), one achieves a much higher precision (better than 1%, see Figure 8) with the following set of parameters:

$$\begin{aligned}\alpha_{\text{n,iso}} &= 0.88, & a_{\text{n,iso}} &= 0.829, \\ \beta_{\text{n,iso}} &= 1.135, & b_{\text{n,iso}} &= 1.27.\end{aligned}\quad (53)$$

Combining Equations (32), (43) and (44) one can determine the temperature-dependence of the emitted photon mean energy:

$$\bar{z}_{\text{ani/iso}} = \frac{1}{E} \frac{\dot{E}_{\text{ani/iso}}}{N_{\text{ani/iso}}} = \frac{F_{\text{ani/iso}}(u)}{F_{\text{n,ani/iso}}(u)} \quad (54)$$

In the case of a mono-directional photon field the argument of the function in the above equation is  $u = 2ET(1 - \cos\theta)$ ; in the case of an isotropic photon field  $u = 4ET$ .

Obviously, the approximate formulae found for functions  $F_{\text{ani}}$ ,  $F_{\text{iso}}$ ,  $F_{\text{n,ani}}$ , and  $F_{\text{n,iso}}$  (see Equations (35), (38), (39), (48), (49), (52), (53)) allow derivation of high-precision analytical formulae for  $\bar{z}$ . However, the 1-parameter freedom in Equations (35) and (38) allows a significant simplification of the expressions. Namely, in the case of a mono-directional photon field, the mean energy can be approximated as

$$\bar{z}_{\text{ani}} = \frac{G_{\text{ani}}^{(0)}}{G_{\text{n,ani}}^{(0)}} \quad (55)$$

with  $c_{z,\text{ani}} \simeq 4.26$  in  $G_{\text{ani}}^{(0)}$  that minimizes the deviation of the approximation function from the precise expression. As seen in Figure 9 the error remains below 3%. Rounding the coefficients to one non-zero digit (i.e., keeping the precision at the level of 10%), one obtains:

$$\bar{z}_{\text{ani}} = \frac{t_\theta}{t_\theta + 0.2} \frac{\log(1 + t_\theta/2)}{\log(1 + 2t_\theta)} . \quad (56)$$

Similarly, for the case of an isotropic photon field, the approximated formula for the fraction of the mean energy,

$$\bar{z}_{\text{iso}} = \frac{G_{\text{iso}}^{(0)}}{G_{\text{n,iso}}^{(0)}}, \quad (57)$$

<sup>3</sup>Here  $\zeta$  denotes the Riemann Zeta-function.

results in a 5% precision (see Figure 9) for the value of  $c_{z,\text{iso}} = 2.9$  in  $G_{\text{iso}}^{(0)}$ . Rounding the coefficients to one non-zero digit one obtains:

$$\bar{z}_{\text{iso}} = \frac{t}{t + 0.3} \frac{\log(1 + t/4)}{\log(1 + t)}. \quad (58)$$

The mean photon energy characterizes the typical energy band of upscattered photons in which an electron loses its energy via IC process. Note that in many cases is more demanded the inverse problem, i.e., a reconstruction of the electron energy on the basis of the observed photon energy and the temperature of the target photons. In other words, one needs to solve the transcendental Equation (58) (or Equation (56)), to obtain  $t$  (or respectively  $t_\theta$ ) as a function of  $\bar{\omega}$  and  $T$ . Using Equations (56) and (58) one can derive the following approximate solution:

$$t_{\theta/\cdot} = \frac{v^{1/2} (1 + 2v^{1/2})}{2} \sqrt{\frac{\log(1 + v^{1/2})}{\log(1 + v^{1/2}/V_0)}}, \quad (59)$$

which allows to obtain the lepton energy with < 10% precision in the entire range of parameters. One should adopt  $V_0 = 3$  and  $v = 2\bar{\omega}T(1 - \cos\theta)$  for the case of mono-directional photon field; and  $V_0 = 4$  and  $v = 4\bar{\omega}T$  for isotropic distribution of photons.

## 5. Impact of relativistic motion

The formulae presented in the previous sections correspond to the reference system, where the source of photons is at rest (we refer this system as  $K$ ). Since the particle distribution can be always transformed to this coordinate system, these formulae can, in principle, cover all the required calculations. However, under certain conditions it is more convenient to perform calculations in another coordinate system,  $K'$  (the physical quantities measured in this system are marked with prime, e.g.  $\omega'_0$ ). In case if the target photons are mono-directional in the reference frame  $K$  (in the relevant region of space), the transformation of the obtained formulae is straightforward. Indeed, in this case the photon distribution function in the 6-dimensional momentum-coordinate phase space ( $dN = \rho d^3\mathbf{p}d^3\mathbf{r}$ ) has the following form:

$$\rho(\mathbf{p}, \mathbf{r}) = \delta(\mathbf{n}_{\mathbf{p}} - \mathbf{n}_0) \frac{c}{p^2} n_{\text{ph}}(\omega_0), \quad (60)$$

where  $\mathbf{n}_{\mathbf{p}} = \mathbf{p}/p$ ,  $\omega_0 = cp$ , and  $\mathbf{n}_0$  is the unit vector corresponding to the direction of photons in the system  $K$ . Function  $n_{\text{ph}}$  corresponds to the energy distribution of the target photons, i.e.,  $dN_{\text{ph}} = n_{\text{ph}}d\omega_0$ , and in the system  $K$  is Planckian. The function  $\rho$  is a Lorentz invariant (see, e.g., Landau & Lifshitz 1975), i.e.,  $\rho(\mathbf{p}, \mathbf{r}) = \rho'(\mathbf{p}', \mathbf{r}')$ , and it can be shown that, in this specific case, the function  $n_{\text{ph}}$  is an invariant as well:

$$n'_{\text{ph}}(\omega'_0) = n_{\text{ph}}(\omega_0). \quad (61)$$

Here target photon energies  $\omega_0$  and  $\omega'_0$  are related via the Lorentz transformation:  $\omega_0 = \mathcal{D}_* \omega'_0$ , where  $\mathcal{D}_* = [\Gamma(1 - (v_0/c) \cos \chi)]^{-1}$  is the Doppler factor between the source of blackbody photons (reference system  $K$ ) and the gamma-ray production region (reference system  $K'$ ) moving with relative velocity  $v_0$ , that makes an angle  $\chi$  to the photon momentum (the variable  $\Gamma = (1 - (v_0/c)^2)^{-1/2}$  denotes the bulk Lorentz factor). Since function  $n_{\text{ph}}(\omega_0)$  in Equation (61) is determined by Equation (4), one can see that in the moving coordinate system  $K'$  the Planckian distribution of photons is preserved, but the temperature of the photon field is corrected for the bulk motion:

$$T' = \mathcal{D}_*^{-1} T, \quad (62)$$

and an additional dilution factor is applied:

$$\kappa' = \mathcal{D}_*^2. \quad (63)$$

Equations (62) and (63) allow a generalization of the formulae obtained in the previous sections for the case of a mono-directional photon field to a moving system  $K'$ . As it follows from their derivations, Equations (60) and (61) do not account for the relativistic effects related to the transformation of the IC emission from the source frame to the observer frame (for detail see, e.g., Rybicki & Lightman 1979; Jester 2008). Also we note that the interaction angle,  $\theta$ , should also be transformed to the system  $K'$ . The transformation of the interaction angle can be readily obtained by considering the scalar product of the 4-momenta of electron and the target photon (i.e., a Lorentz invariant quantity). Finally, in the case when the emitting particles are isotropized in the reference frame  $K'$ , the energy loss rate is described by Equation (36) with corrections imposed by Equations (62) and (63).

We leave out of the scope of this paper the transformation of a photon field isotropic in the system  $K$  to the moving system  $K'$ . If looked from the system  $K'$ , such a photon field is not isotropic field, therefore the basic equation Equation (3) is not applicable for description the IC scattering process. If the bulk Lorentz factor is large,  $\Gamma \gg 1$ , the photon field in the  $K'$  system appears to be nearly mono-directional, with photons moving against the bulk velocity. But the energy distribution of the photons in this case deviates significantly from the Planckian distribution. We note however that in the case of an isotropic photon field, the distribution of electrons can be transformed to the system  $K$  and the formulae obtained for the spectrum can be used.

## 6. Comparison with other approaches

In order to simplify calculations, one may try to replace the relatively narrow Planckian distribution by the  $\delta$ -function, or alternatively use a simplified description of the cross-section, e.g., by the Heaviside step function (Petruk 2009) or simply by a  $\delta$ -function. For the sake of shortness, in what follows we discuss the  $\delta$ -functional approximation for a mono-directional target photon field, and the step function approximation by Petruk (2009) for the scattering off isotropic photon field.

The  $\delta$ -functional approximation for target photons assumes the following photon field:

$$\frac{dN_{\text{ph}}}{d\omega_0} \simeq n_* \delta(\omega_0 - \omega_*). \quad (64)$$

It is easy to be convinced that for  $n_* = \frac{2\zeta(3)m_e^3 c^3 \kappa T^3}{\pi^2 \hbar^3}$  and  $\omega_* = \frac{\pi^4}{30\zeta(3)} T \simeq 2.7 T$  one can reproduce correctly both the number and energy densities of the Planckian photon field. However, to a certain extent, the choice of these parameters is arbitrary.

The substitution of Equation (64) into Equation (7) results in the following expression:

$$\frac{dN_{\text{ani}}}{d\omega dt} = \frac{2r_o^2 m_e^3 c^4 \kappa T^2}{\pi \hbar^3 E^2} \times \left[ \frac{z^2}{2(1-z)} G_{1,\delta}(x_0) + G_{2,\delta}(x_0) \right], \quad (65)$$

where

$$G_{1,\delta}(x_0) = \frac{n_* \hbar^3 \pi^2}{\kappa T^2 \omega_* m_e^3 c^3} \Theta\left(\frac{\omega_*}{T} - x_0\right), \quad (66)$$

and

$$G_{2,\delta}(x_0) = \frac{n_* \hbar^3 \pi^2}{\kappa T^2 \omega_* m_e^3 c^3} \Theta\left(\frac{\omega_*}{T} - x_0\right) \times \left(1 - \frac{2x_0}{\omega_*/T} + \frac{2x_0^2}{(\omega_*/T)^2}\right). \quad (67)$$

Here  $\Theta(x_0)$  is the Heaviside step function.

The comparison of Equations (66) and (12), and of Equations (67) and (13), allows us to estimate the errors introduced by the  $\delta$ -functional approximation: (1) the lower energy part of the spectrum ( $x_0 \ll 1$ ) can be reproduced quite well if the selected parameters satisfy the condition  $n_*/(T^2 \omega_*) = \kappa m_e^3 c^3 / (6\hbar^3)$ ; (2) the accuracy declines significantly for the high energy part ( $x_0 \gtrsim 1$ ). The  $\delta$ -function imposes an artificial cutoff at  $x_0 = \omega_*/T$ . Also the accuracy close to the cutoff appears to be quite poor. For example, the accuracy of the term  $G_{1,\delta}$  can be estimated as  $G_{1,\delta}/G_1^{(0)}$  which gives a factor of 3 error for  $x_0 = 2$  (assuming that  $\omega_*/T > 2$ , as commonly adopted).

Similarly, it can be shown that for the cross section averaged over the interaction angle, the  $\delta$ -functional approximation gives a similar precision. It means that although a practical realization of the  $\delta$ -functional approximation is characterized by a similar complexity as the approach suggested in this paper, the accuracy provided by the  $\delta$ -functional approximation is very poor, especially in the Klein-Nishina regime.

A more complicated approach has been suggested by Petruk (2009) for the case of the cross section averaged over the interaction angle. In this approach the IC cross section was approximated by a step function and integrated over the Planckian photon distribution. This approximation, can be expressed as

$$\frac{dN_{\text{iso}}}{d\omega dt} = \frac{2r_o^2 m_e^3 c^4 \kappa T^2}{\pi \hbar^3 E^2} \times \left[ \frac{z^2}{2(1-z)} G_{3,\text{p}}(x_0) + G_{4,\text{p}}(x_0) \right], \quad (68)$$

where

$$G_{3,\text{p}}(x_0) = \frac{\pi^2}{6} e^{-\frac{2}{3}x_0 - \frac{5}{7}x_0^{0.7}}, \quad (69)$$

and

$$G_{4,\text{p}}(x_0) = \frac{\pi^2}{6} e^{-\frac{2}{3}x_0 - \frac{5}{4}x_0^{0.5}}. \quad (70)$$

In Figure 10 we compare the approximation of Petruk (2009) with precise numerical calculations, and arrive at a conclusion, similar to the statement of Zdziarski & Pjanka (2013), that for certain parameters this approximation cannot guaranty a precision better than  $\sim 50\%$  (we note that Petruk 2009, did not approximate the cross section in the region of the exponential tail, i.e. for  $x_0 \gg 1$ ).

Finally, Zdziarski & Pjanka (2013) suggested an analytical method to describe Equations (2) and (3) based on the truncation of series, which describe the functions  $f_{-1}$  and  $f_{\text{in}}$ . In Figure 11 we compare precise numerical calculations to the approximated values,  $G_{3,z}$  and  $G_{4,z}$ , that were obtained by substitution of Equations (7), (8), (14), and (28) from Zdziarski & Pjanka (2013) (the value of  $N = 3$ , as suggested by the authors, was adopted) to Equations (15) and (16). Since Zdziarski & Pjanka (2013) obtained analytical expressions for the functions  $f_{+1}$  and  $f_0$ , the function  $G_{3,z}$  is strictly equal to  $F_3$ , which can be seen in Figure 11. The accuracy provided by the function  $G_{4,z}$  is very high, at the level of  $0.3\%^4$  (see Figure 11).

The approach by Zdziarski & Pjanka (2013) can provide an arbitrary precision (simply by increasing of the number the preserved terms in the series), however, in our view, it also owns a certain shortcoming. Namely, this approach implies the usage of special functions (dilogarithm and exponential integral), which may harden the practical usage.

Another important difference of our approach is that while in other studies one provides an approximate description for the cross section, we suggest an approach for a common description of all the relevant processes of IC scattering on the black-body photons: scattering rates, energy losses, cross sections and mean photon energy. Also, all the approximations use the same type of correction function, Equation (20).

---

<sup>4</sup> This accuracy is worse by approximately a factor of 10 than the accuracy of  $< 2.4 \times 10^{-4}$  achieved for the functions  $f_{-1}$  and  $f_{\text{in}}$  (Zdziarski & Pjanka 2013). This discrepancy is explained by the fact that these functions enter into the expression for the cross section with different signs, and the subtraction of these functions results in an overall error significantly exceeding the accuracy of the individual terms.

## 7. Summary

In this paper we suggest simple analytical presentations for calculations of different characteristics (differential spectra, interaction rates, and energy losses) of the IC scattering of relativistic electrons in the radiation field which is described by Planckian distribution. Two different types of angular distribution, namely mono-directional and isotropic distributions of the target radiation field have been considered.

The obtained parameterizations are characterized by a high precision, of an order of 1%, and cover the entire parameter space allowing an accurate description of the IC scattering in the Thomson and Klein-Nishina limits, as well as in the transition region. The derived formulae preserve the precise asymptotic behavior and have similar structures, which simplifies their practical usage (see Table 1).

The main objective of the obtained approximate analytical presentations is the fast, but convenient and accurate calculations of characteristics of the upscattered IC emission in radiation fields described by Planckian distribution. At the same time, the simple forms of these parameterizations allow derivation of some useful relations. In particular, we propose simple formulae which, for the given temperature of target photons, relate the mean energy of the electron and up-scattered photon.

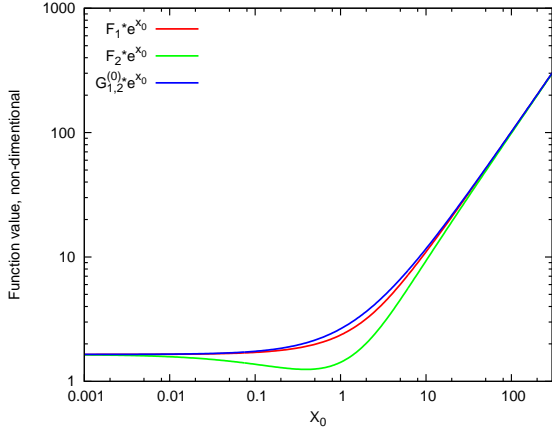


Fig. 1.— Functions  $F_1$ ,  $F_2$  are shown together with the zeroth-order approximation  $G_1^{(0)}$  (the function  $G_2^{(0)}$  is equal to  $G_1^{(0)}$ ). The function  $G_1^{(0)}$  reproduces asymptotic behavior of functions  $F_{1,2}$ , but differs by a factor  $\lesssim 2$  for  $x_0 \sim 1$ .

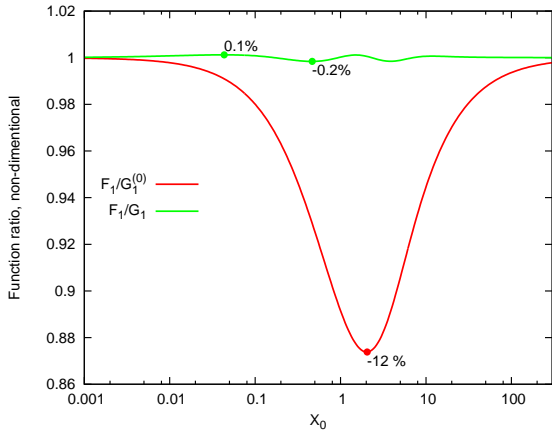


Fig. 2.— The ratios of function  $F_1$  to approximations  $G_1^{(0)}$  and  $G_1$ .

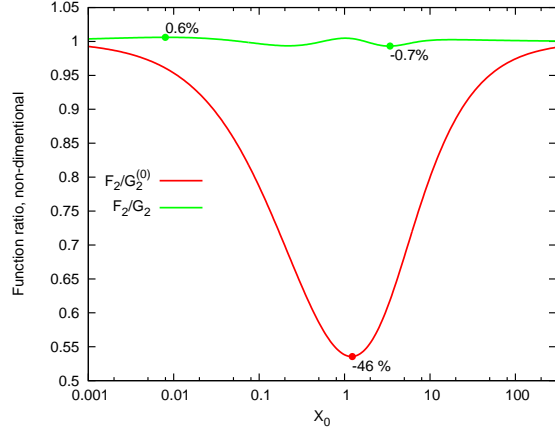


Fig. 3.— The ratios of function  $F_2$  to approximations  $G_2^{(0)}$  and  $G_2$ .

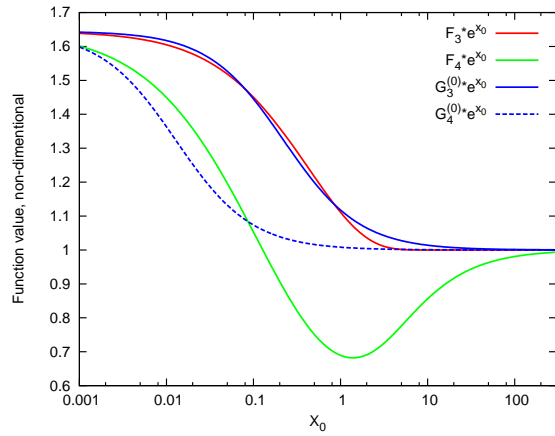


Fig. 4.— Functions  $F_3$ ,  $F_4$  are shown together with the zeroth-order approximations  $G_3^{(0)}$ , computed for  $c_3 = 2.73$ , and  $G_4^{(0)}$ , computed for  $c_4 = 47.1$ .

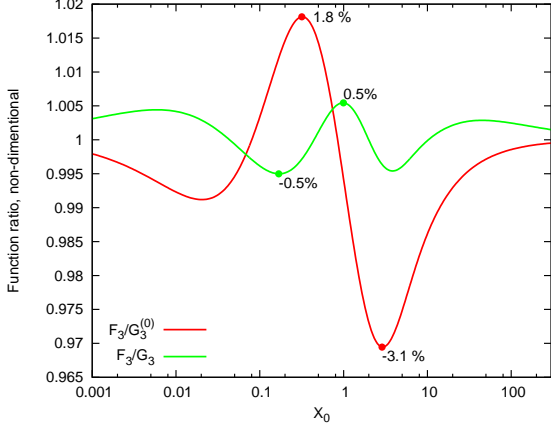


Fig. 5.— The ratios of function  $F_3$  to approximations  $G_3^{(0)}$  (taken for  $c_3 = 2.73$ ) and  $G_3$ . The used fitting parameters are shown by Equation (26).

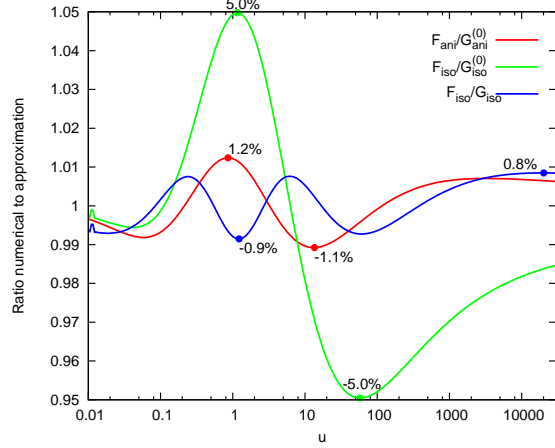


Fig. 7.— The ratio of the function  $F_{\text{ani}}$  to  $G_{\text{ani}}^{(0)}$  (for  $c_{\text{ani}} = 6.13$ ) and  $F_{\text{iso}}$  to  $G_{\text{iso}}^{(0)}$  (for  $c_{\text{iso}} = 4.62$ ) and  $G_{\text{iso}}^{(0)} \times g(u)$ .

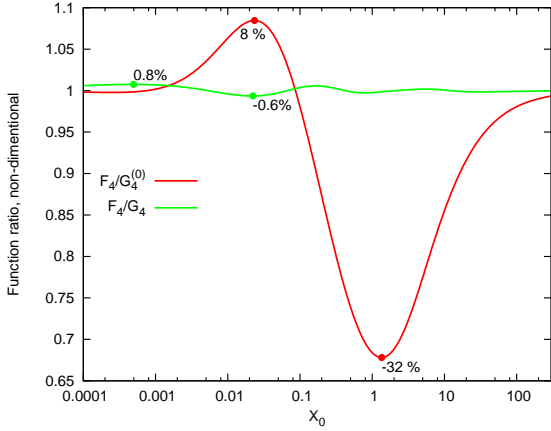


Fig. 6.— The ratios of the function  $F_4$  to approximations  $G_4^{(0)}$  (taken for  $c_4 = 47.1$ ) and  $G_4$ . We show this plot for increased range of  $x_0$ , as compared to Figures 1 – 5, to include the region where the ratio of  $F_4$  to  $G_4$  achieves its maximum.

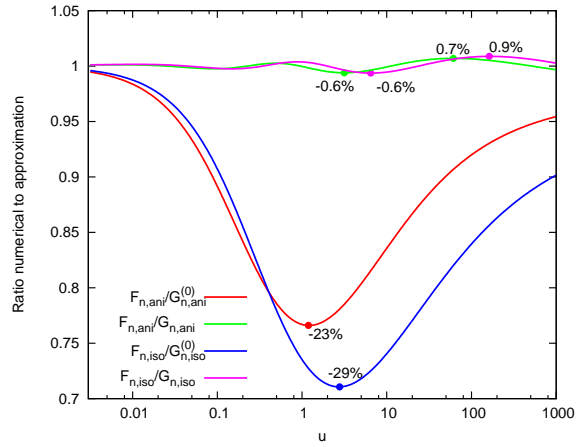


Fig. 8.— The ratios of the function  $F_{n,\text{ani}}$  to  $G_{n,\text{ani}}^{(0)}$  and to  $G_{n,\text{ani}}^{(0)} \times g(u)$ ; and the ratios of the function  $F_{n,\text{iso}}$  to  $G_{n,\text{iso}}^{(0)}$  and to  $G_{n,\text{iso}}^{(0)} \times g(u)$ .

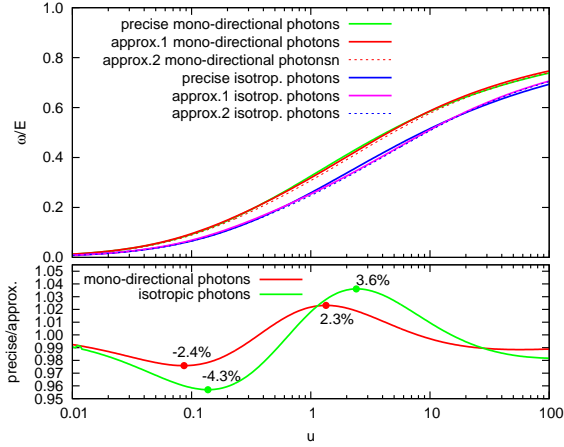


Fig. 9.— Upper panel: The ratio of the mean energy of the upscattered photon to the electron energy plotted as a function of  $u = t$  (for isotropic photon field) and  $u = t_\theta$  (for mono-directional photon field). The approximation 1 corresponds to Equations (55) and (57) for the cases of mono-directional and isotropic photon fields, respectively. The approximation 2 corresponds to Equations (56) and (58) for the cases of mono-directional and isotropic photon fields, respectively. Bottom panel: ratios of numerical calculations to approximations given by Equations (55) and (57) for the cases of mono-directional and isotropic photon fields, respectively.

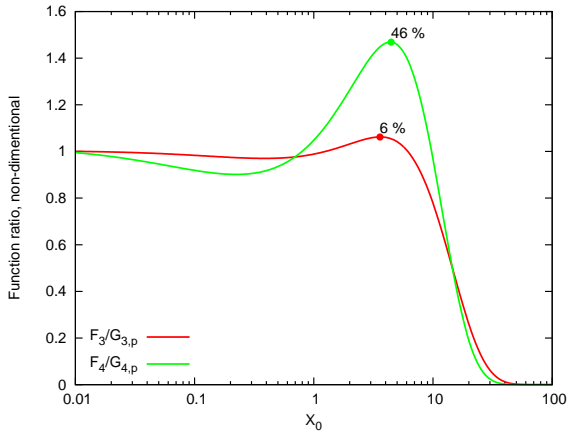


Fig. 10.— Comparison of the approximation proposed by Petruk (2009) to the numerical calculations.

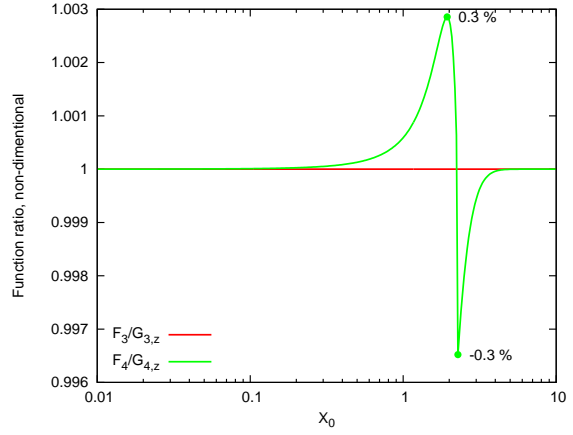


Fig. 11.— Comparison of the approximation proposed by Zdziarski & Pjanka (2013) to the numerical calculations.

## REFERENCES

- Aharonian, F., et al. 2006, *A&A*, 460, 743
- Aharonian, F. A., & Atoyan, A. M. 1981, *Ap&SS*, 79, 321
- Berestetskii, V. B., Lifshitz, E. M., & Pitaevskii, L. P. 1971, *The Classical Theory of Fields* (Pergamon Press, Oxford)
- Blumenthal, G. R., & Gould, R. J. 1970, *Reviews of Modern Physics*, 42, 237
- Bosch-Ramon, V., & Khangulyan, D. 2009, *International Journal of Modern Physics D*, 18, 347
- Jester, S. 2008, *MNRAS*, 389, 1507
- Jones, F. C. 1968, *Physical Review*, 167, 1159
- Khangulyan, D., Aharonian, F. A., Bogovalov, S. V., & Ribó, M. 2011, *ApJ*, 742, 98
- Khangulyan, D., Hnatic, S., Aharonian, F., & Bogovalov, S. 2007, *MNRAS*, 380, 320
- Landau, L. D., & Lifshitz, E. M. 1975, *The Classical Theory of Fields* (Pergamon Press, Oxford)
- Petruk, O. 2009, *A&A*, 499, 643
- Rybicki, G. B., & Lightman, A. P. 1979, *Radiative Processes in Asrtophysics* (New Yprk: Wiley)
- Zdziarski, A. A., & Pjanka, P. 2013, *MNRAS*, 436, 2950

TABLE 1  
DERIVED PARAMETERIZATIONS

Function	Used in Eqs.	Approximated description		Fit parameters values				precision	Figure	
		function	variable	$a$	$\alpha$	$b$	$\beta$			$c$
Representation of Spectra										
$F_1$	Eq. (11)	$G_1^{(0)} = \left(\frac{\pi^2}{6} + x_0\right) e^{-x_0}$	$\frac{z}{1-z} \frac{1}{2ET(1-\cos\theta)}$	—	—	—	—	—	$\sim 10\%$	Figs. 1,2
$F_1$	Eq. (11)	$G_1^{(0)}(x_0) \times g(x_0)$	$\frac{z}{1-z} \frac{1}{2ET(1-\cos\theta)}$	0.153	0.857	0.254	1.84	—	$< 1\%$	Figs. 1,2
$F_2$	Eq. (11)	$G_2^{(0)} = \left(\frac{\pi^2}{6} + x_0\right) e^{-x_0}$	$\frac{z}{1-z} \frac{1}{2ET(1-\cos\theta)}$	—	—	—	—	—	$\sim 50\%$	Figs. 1,3
$F_2$	Eq. (11)	$G_2^{(0)}(x_0) \times g(x_0)$	$\frac{z}{1-z} \frac{1}{2ET(1-\cos\theta)}$	1.33	0.691	0.534	1.668	—	$< 1\%$	Figs. 1,3
$F_3$	Eq. (14)	$G_3^{(0)} = \frac{\pi^2}{6} \frac{1+c x_0}{1+\frac{c}{6} x_0} e^{-x_0}$	$\frac{z}{1-z} \frac{1}{4ET}$	—	—	—	—	2.73	$\sim 3\%$	Figs. 4,5
$F_3$	Eq. (14)	$G_3^{(0)}(x_0) \times g(x_0)$	$\frac{z}{1-z} \frac{1}{4ET}$	0.443	0.606	0.54	1.481	0.319	$< 1\%$	Figs. 4,5
$F_4$	Eq. (14)	$G_4^{(0)} = \frac{\pi^2}{6} \frac{1+c x_0}{1+\frac{c}{6} x_0} e^{-x_0}$	$\frac{z}{1-z} \frac{1}{4ET}$	—	—	—	—	47.1	$\sim 30\%$	Figs. 4,6
$F_4$	Eq. (14)	$G_4^{(0)}(x_0) \times g(x_0)$	$\frac{z}{1-z} \frac{1}{4ET}$	0.726	0.461	0.382	1.457	6.62	$< 1\%$	Figs. 4,6
Energy Losses										
$F_{\text{ani}}$	Eq. (33, 55)	$G_{\text{ani}}^{(0)} = \frac{cu \log(1+2.16u/c)}{1+cu/0.822}$	$2ET(1 - \cos\theta)$	—	—	—	—	6.13	$\sim 1\%$	Fig. 7
$F_{\text{iso}}$	Eq. (36, 57)	$G_{\text{iso}}^{(0)} = \frac{cu \log(1+0.722u/c)}{1+cu/0.822}$	$4ET$	—	—	—	—	4.62	$\sim 5\%$	Fig. 7
$F_{\text{iso}}$	Eq. (36)	$G_{\text{iso}}^{(0)}(u) \times g(u)$	$4ET$	-0.362	0.682	0.826	1.281	5.68	$\sim 1\%$	Fig. 7
Interaction Rate										
$F_{\text{n,ani}}$	Eq. (46, 55)	$G_{\text{n,ani}}^{(0)} = 0.822 \log(1 + 1.949u)$	$2ET(1 - \cos\theta)$	—	—	—	—	—	$\sim 25\%$	Fig. 8
$F_{\text{n,ani}}$	Eq. (46)	$G_{\text{n,ani}}^{(0)}(u) \times g(u)$	$2ET(1 - \cos\theta)$	1.05	0.885	2.46	1.213	—	$\sim 1\%$	Fig. 8
$F_{\text{n,iso}}$	Eq. (50, 57)	$G_{\text{n,iso}}^{(0)} = 0.822 \log(1 + 0.97u)$	$4ET$	—	—	—	—	—	$\sim 30\%$	Fig. 8
$F_{\text{n,iso}}$	Eq. (50)	$G_{\text{n,iso}}^{(0)}(u) \times g(u)$	$4ET$	0.829	0.88	1.27	1.135	—	$\sim 1\%$	Fig. 8
Mean Energy of Emitted Photons										
$\bar{z}_{\text{ani}}$	Eq. (55)	$G_{\text{ani}}^{(0)}/G_{\text{n,ani}}^{(0)}$	$2ET(1 - \cos\theta)$	—	—	—	—	4.26	$\sim 3\%$	Fig. 9
$\bar{z}_{\text{ani}}$	Eq. (56)	$\frac{u}{u+0.2} \frac{\log(1+u/2)}{\log(1+2u)}$	$2ET(1 - \cos\theta)$	—	—	—	—	—	$\sim 8\%$	Fig. 9
$\bar{z}_{\text{iso}}$	Eq. (57)	$G_{\text{iso}}^{(0)}/G_{\text{n,iso}}^{(0)}$	$4ET$	—	—	—	—	2.9	$\sim 5\%$	Fig. 9
$\bar{z}_{\text{iso}}$	Eq. (58)	$\frac{u}{u+0.3} \frac{\log(1+u/4)}{\log(1+u)}$	$4ET$	—	—	—	—	—	$\sim 8\%$	Fig. 9
Energy of Emitting Particle										
$t_\theta$	Eq. (59)	$\frac{v^{1/2}(1+2v^{1/2})}{2} \sqrt{\frac{\log(1+v^{1/2})}{\log(1+v^{1/2}/3)}}$	$2\bar{\omega}T(1 - \cos\theta)$	—	—	—	—	—	$\sim 10\%$	—
$t$	Eq. (59)	$\frac{v^{1/2}(1+2v^{1/2})}{2} \sqrt{\frac{\log(1+v^{1/2})}{\log(1+v^{1/2}/4)}}$	$4\bar{\omega}T$	—	—	—	—	—	$\sim 10\%$	—

NOTE.—A typical parametrization consists of a zeroth-order approximation function,  $G_{\dots}^{(0)}$ , multiplied by the correction factor  $g$ . The zeroth-order approximation depends on the variable, which is listed in the fourth column of the table, and in some cases on the parameter  $c$ . The correction factor is given by Equation (20), and depends on the same variable as the zeroth-order approximation, and four parameters ( $a$ ,  $\alpha$ ,  $b$  and  $\beta$ ).